THE JOURNAL OF PHYSICAL CHEMISTRY Letters

Letter

pubs.acs.org/JPCL

# Gas-Phase Neutral Binary Oxide Clusters: Distribution, Structure, and Reactivity toward CO

Zhe-Chen Wang, Shi Yin, and Elliot R. Bernstein*

Department of Chemistry, NSF ERC for Extreme Ultraviolet Science and Technology, Colorado State University, Fort Collins, Colorado 80523, United States

Supporting Information

**ABSTRACT:** Neutral binary (vanadium−cobalt) oxide clusters are generated and detected in the gas phase for the first time. Their reactivities toward carbon monoxide (CO) are studied both experimentally and theoretically. Experimental results suggest that neutral $VCoO_4$ can react with CO to generate $VCoO_3$ and $CO_2$. Density functional theory studies show parallel results as well as provide detailed reaction mechanisms.

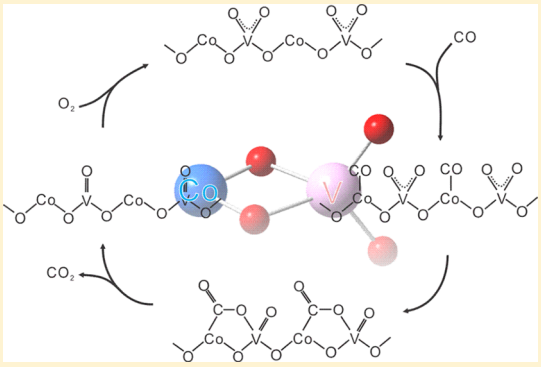


**SECTION:** Kinetics and Dynamics

Vanadium-containing supported catalysts are widely employed in many chemical reactions,[1] due to their efficient performance in various catalytic processes: carbon monoxide (CO) oxidation,[2] oxidative dehydrogenation (ODH) of alkanes,[3,4] and dehydrosulfurization of aromatic substances.[5] Recent studies show that the coexistence of $V^{5+/4+}$ and $Co^{3+/2+}$ sites on vanadium−cobalt (V−Co) oxide catalysts should be an important factor for high selectivity in ODH of ethane ($C_2H_6$) and that cobalt can modify the redox behavior of vanadium.[3] Correspondingly, vanadium species doped in an appropriate amount can cause disorder in the spinel structure of cobalt chromites, thus favoring oxygen mobility and promoting catalytic performance for methane ($CH_4$) combustion.[6] Nevertheless, the precise description of the "active sites" existing on the surface of $VO_x$/supported catalysts is still a challenge, and conflicting conclusions have been drawn from the available surface-characterization methods applied.[7,8]

An ideal model system to simulate real surface reactions and to discover surface reaction mechanisms is gas-phase clusters in an "isolated" environment.[9,10] Many excellent studies have been accomplished with regard to the structure and reactivities of gas-phase cationic,[9,11−21] anionic,[12,22−27] and neutral[28−33] metal oxide clusters (NMOCs). Employing NMOCs for the study of catalytic processes is advantageous as it minimizes the effect of cluster charge, which has been considered to be significant with regard to cluster reactivity.[21,34,35]NMOCs often have high vertical ionization energies (>8 eV), and multiphoton ionization with a 10 ns $Nd^{3+}$/YAG laser pulse can cause significant cluster fragmentation and confuse the mass spectra for reactants and products.[36,37]

Recently, our group has developed a novel 118 nm, single-photon ionization (SPI) technique, which has proved to be reliable for detecting the distribution and reactivity of NMOCs without dissociation.[38−40] Many gas-phase NMOCs and their reactivities have been studied in recent years (e.g., the reactions of vanadium-, cobalt-, iron-, and tantalum-containing NMOCs with CO,[41] ethylene,[32,42] propylene,[42,43] acetylene,[32] sulfur dioxide,[44] ammonia,[45] and methanol[31]). These cluster studies yield an understanding of the corresponding real catalytic systems and enable one to propose a full catalytic cycle at the molecular level for the bulk catalytic system.

In the past few years, the study of binary metal oxide clusters (BMOCs) has been reported for ionic systems. These cluster systems can serve as a more detailed molecular approach for the understanding of the active sites in catalytic supports and modified catalytic systems.[17,19,20,23,35,46−52] The first example of generating, as well as studying, the reactivity of BMOCs is reported by He and coworkers. They proposed that the novel $AlVO_4^+$ cluster can activate $CH_4$ oxidation at room temperature.[20] Additionally, Schwarz and coworkers and He and coworkers reported $CH_4$ activation by $V_3PO_{10}^+$ with different cluster generating methods at almost the same time.[47,50] The Schwarz group also illustrated the first complete gas-phase catalytic cycle conducted by the BMOC $AlVO_3^+/AlVO_4^+$ couple through both experimental and theoretical studies.[19] Sauer, Asmis, and coworkers studied the infrared spectroscopy

**Received:** June 26, 2012
**Accepted:** August 16, 2012
**Published:** August 16, 2012

  

of $CeVO_4^+$, $CeV_2O_6^+$, and $Ce_2VO_5^+$ BMOCs for the first time, indicating interesting structures parallel to the condensed phase $VO_x/CeO_2$ supported materials.[17] The initial studies of the photoelectron spectroscopy of BMOCs are reported by Zheng and coworkers, whose group investigated $MAlO_x^-$ and $M_xAlO_2^-$ (M = Ti or V; $x$ = 1, 2, or 3) BMOCs. These experimental mass resolved results are coupled to density functional theory (DFT) calculations to provide insight into the electronic properties of supported vanadium and titanium oxides.[23,51]

Despite the importance of BMOCs for catalysis, to the best of our knowledge, experimental and theoretical studies on the reactivity of neutral binary metal oxide clusters (NBMOCs) have not been reported. This letter reports the generation of V−Co NBMOCs and the study of their reactivities toward CO.

Figure 1 shows the distribution of V−Co NBMOCs detected by 118 nm SPI and time-of-flight mass spectrometry

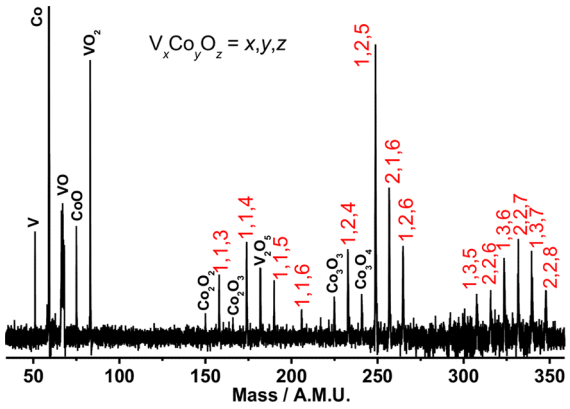


**Figure 1.** Distribution of V−Co NBMOCs detected by SPI TOFMS at 118 nm.

(TOFMS). The distribution is generated by laser ablation of V/Co metal disk with 0.5% $O_2$ seeded in helium carrier gas. The series $V_xCo_yO_z$, (with $x + y$ = 2−4; that is, $VCoO_{3-6}$, $VCo_2O_{4-6}$, $V_2CoO_6$, $VCo_3O_{5-7}$, and $V_2Co_2O_{6-8}$) can be observed.

The reaction of V−Co NBMOCs with CO is shown in Figure 2. The mass spectrum is very sensitive to experimental conditions, and the two curves in Figure 2 are recorded under well-controlled "identical" conditions, except for the introduction of CO for the red curve. The intensity of the signal for

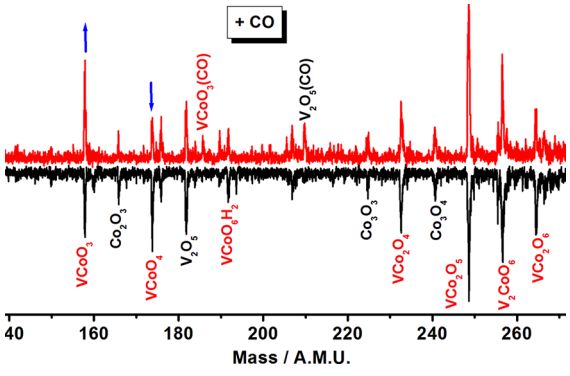


**Figure 2.** Reaction of V−Co NBMOCs with pure CO. The blue arrows point out the decrease in the $VCoO_4$ signal and the corresponding increase in the $VCoO_3$ signal when CO added into the reaction cell.

$VCoO_4$ decreases with increasing $VCoO_3$ when CO is added to the fast flow reaction cell, to generate reaction 1

$$VCoO_4 + CO \rightarrow VCoO_3 + CO_2, \quad \Delta E = -1.35 \text{ eV} \qquad (1)$$

The ratio of the intensities of $VCoO_3$ to $VCoO_4$ in Figures 1 and 2 is not exactly the same for the reference spectra due to fluctuations in the relative signal intensities and variations in the growth and cooling conditions in the experiment from day to day. This is also true for the background noise signal, as can be seen in the Figures. In Figure 1, the $VCoO_3/VCoO_4$ signal ratio is 0.98/1.52 = 0.64, and in Figure 2 the before reaction signal ratio for $VCoO_3/VCoO_4$ is 0.99/1.25 = 0.79. This is certainly within reason for the small signals and is typical day-to-day experimental variation: 0.64 to 0.79 or 0.72 ± 0.08 seems quite reasonable. This ratio, after the reaction experiment with CO, is (1.56 + 0.25)/0.57 = 3.18 ± 0.2: the variation range comes from separate experiments and the background noise signals. Other signal (e.g., $VCoO_3(CO)$) intensities contribute to reducing the above ratio (by as much as 0.25). Therefore, even though the quantitative signal ratio value is not without some uncertainty, the overall qualitative result is clear: the $VCoO_3/VCoO_4$ intensity ratio before and after reaction has changed by at least a factor of 4 due to the $VCoO_4 + CO \rightarrow VCoO_3 + CO_2$ reaction. Other reactions are evident, such $VCoO_3 + CO \rightarrow VCoO_3(CO)$, as well. The total abundance of $VCoO_3$, $VCoO_4$, and $VCoO_3CO$ (2.38) in Figure 2 after the reaction is ∼6% more than that of the unreacted $VCoO_3$ and $VCoO_4$ before the reaction (2.24): well within the inevitable system fluctuation for weak signals.

Reaction 1 is exothermic according to DFT calculations ($\Delta E$, zero-point energy corrected reaction enthalpy at 0 K). The concentration of CO is estimated to be more than $10^5$ times that of free $VCoO_4$ in the reaction, so we can treat reaction 1 as a pseudo-first-order reaction. The pseudo-first-order reaction constant ($k$) in the fast flow reactor can be estimated by using the following equations:[20,41]

$$I = I_0 \exp(-k\rho l/v) \qquad (2)$$

in which $I$ and $I_0$ are signal magnitudes of the clusters in the presence and absence of reagent gas; $\rho$ is the molecular density of reactant gas; $l$ is the effective path length of the reactor, and $v$ is the cluster beam velocity. The estimated rate constant for reaction 1 is on the order of $10^{-11}$ $cm^3$ $molecule^{-1}$ $s^{-1}$ according to our experimental results with an uncertainty of ±50%.

The CO absorption products $VCoO_3(CO)$ and $V_2O_5(CO)$ can also be observed in Figure 2.

$$VCoO_3 + CO \rightarrow VCoO_3(CO) \qquad (3)$$

$$V_2O_5 + CO \rightarrow V_2O_5(CO) \qquad (4)$$

Although $V_2O_5(CO)$ is formed as a result of CO attachment to $V_2O_5$, the intensity of $V_2O_5$ signal after the reaction is almost the same as the intensity of the unreacted $V_2O_5$ reference signal. Two possible reasons for this behavior can be suggested: (1) system fluctuations mentioned above and/or (2) ionization efficiency of $V_2O_5(CO)$ is possibly higher, which will lead to a higher signal. (See the similar result for the generation of $V_2O_5(C_2H_6)$ in the reaction of $V_2O_5 + C_2H_6$ in ref 32.) Other less significant reactions for CO to $CO_2$ can be mentioned for couples such as $VCo_2O_6/VCo_2O_5$, all of which can contribute to variations in the exact ratios for particular couples before and


dx.doi.org/10.1021/jz3008276 | J. Phys. Chem. Lett. 2012, 3, 2415−2419

after the CO to $CO_2$ reaction, especially for the possible $V_xCo_yO_z(CO)_n$ clusters.

Figure 3 shows the DFT-optimized most stable structures of $VCoO_4$ (**1**) and $VCoO_3$ (**2**). (See the Supporting Information

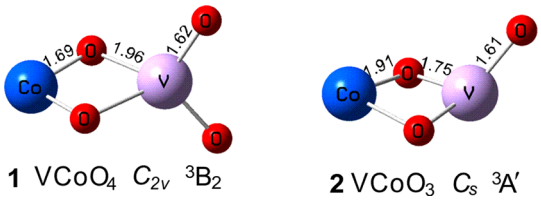


**Figure 3.** Optimized ground-state structures of $VCoO_3$ and $VCoO_4$ using a DFT BPW91/TZVP algorithm.

for other isomers.) The structure of $VCoO_3$ (**2**) in the triplet ground state is kite-shaped within the $C_s$ point group. This structure is similar to that for the neutral $V_2O_3$ cluster,[53] substituting Co for V at the two-oxygen-coordinated position. According to our calculation, the $VCoO_4$ (**1**, triplet) is the isomer of $VCoO_4$ with the lowest energy. (See Figure 3.) The geometry of the triplet $VCoO_4$ (**1**, triplet) is in a $C_{2v}$ point group with the $CoO_bO_bVO_tO_t$ ($O_b$, bridged oxygen; $O_t$, terminal oxygen) structure, which is different from the *trans*-$O_tVO_bO_bVO_t$ structure of $V_2O_4$.[53] Another isomer of $VCoO_4$ (**6**, triplet, see Supporting Information), which is only 0.03 eV higher in energy than $VCoO_4$ (**1**, triplet), is present. We also calculate the potential energy reaction surface for the $VCoO_4$ (**6**, triplet) structure with CO and find that this reaction is also barrierless. (See the Supporting Information.) Therefore, the overall conclusion does not change despite the structural complexity of $VCoO_4$. (See the following text for the details.)

Because the Co−O and V−O bridging distances change significantly from structures **1** to **2**, the oxidation states change for the Co and V sites in these clusters. We determine charges for Co and V in their clusters employing electrostatic potentials using a grid-based method (CHELPG)[54] for V and Co in both $VCoO_4$ (**1**) and $VCoO_3$ (**2**). The charge values for Co change from 1.68 for **1** to 1.28 for **2**, indicating a significant oxidation state variation. The charge values for V change a little from 2.21 for **1** to 2.14 for **2**.

Reaction 1 involves an O-atom transfer from $VCoO_4$ to CO. The calculated potential energy surface for this process, as shown in Figure 4, reveals that the favorable oxidation proceeds

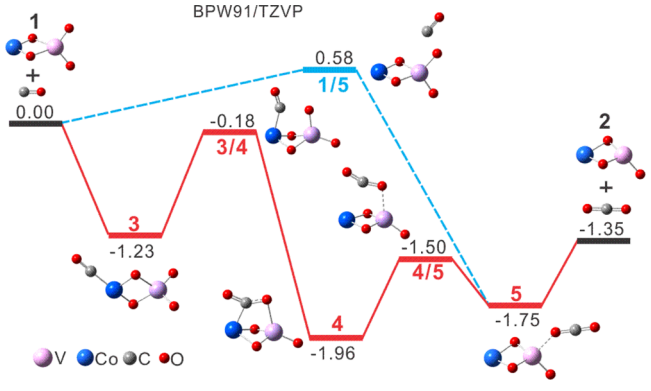


**Figure 4.** Triplet potential energy surface for the reaction of $VCoO_4$ with CO. The *E* values are relative to the entrance channel, corrected with zero-point energy, and given in electronvolts.

by an initial bonding of the carbon atom of CO on the Co site of the $CoO_bO_b$ moiety to form the $(CO)CoO_bO_bVO_tO_t$ encounter complex, intermediate **3**. Co binding to the C atom of CO rather than the O atom is typically rationalized by a mechanism that suggests electron donation from the HOMO of CO ($\pi$) to the empty metal d orbital and electron back-donation from the filled metal d orbital to the CO ($\pi^*$) LUMO. The initial process releases 1.23 eV binding energy, which provides enough energy for the following $CO_2$ moiety formation process (**3** → **3/4** → **4**). Then, the C atom attacks one of the $O_t$ atoms at the $VO_tO_t$ side (transition state **3/4**), resulting in a stable intermediate **4** with a bridging $CO_2$ moiety (Figure 4). The elongation of Co−C bond takes place easily to form a linear $CO_2$ moiety (**4** → **4/5** → **5**). Note that the linear $CO_2$ unit is fully located on the V site instead of Co site in intermediate **5**. The dissociation of $CO_2$ from intermediate **5** leads to the final products $VCoO_3$ and $CO_2$ formation.

We also consider the approaching of CO directly to one of the $O_t$ atoms of $VO_tO_t$ moiety. This approach, transition state **1/5** in Figure 4, has a significant barrier and is thus unfavorable for the reaction processes.

The reactions of neutral cobalt oxide clusters with CO have been reported recently, and $Co_3O_4$ is suggested to be very reactive toward CO.[30] The first CO combination step for $Co_3O_4$ + CO is very similar to that of $VCoO_4$ + CO, and the C-atom end of CO is chemically absorbed on the Co site. Subsequently, the oxygen-transfer process in the $Co_3O_4$/CO system involves one $O_b$ atom between two Co atoms, which is different from that of $VCoO_4$/CO system with only $O_t$ on the V site involved.

$AlVO_4^+$ and $VCoO_4$ are both stoichiometric BOCs that are active to CO.[19] Unlike the neutral $VCoO_4$/CO cluster, the cationic $AlVO_4^+$ reacts with CO more straightforwardly. For the $AlVO_4^+$/CO cluster, the carbon atom of CO approaches directly the terminal oxygen of the $O_bO_bAlO_t$ moiety combined with a large amount of energy release: the reaction rate is also about one order faster than that of $VCoO_4$/CO.[19] This comparison reveals that both the charge effect and the spin distribution play important roles in the chemistry because the only unpaired electron of $AlVO_4^+$ is located on the $O_t$ atom of the $O_bO_bAlO_t$ moiety while the Co atom of $VCoO_4$ possesses a Mulliken atomic spin density of 1.46.

V−Co binary oxide catalysts have been widely used on ODH of alkanes.[3,55] Both V- or Co-doped oxides provide high performance for CO oxidation.[2] The activities of V−Co oxide catalysts highly depend on the coexistence as well as interaction of $V^{5+/4+}$ and $Co^{3+/2+}$ sites.[3] The gas-phase cluster $VCoO_4$ provides a more clear and perhaps ideal mechanism for the CO oxidation by a real V−Co oxide surface: (1) CO is chemically absorbed on the Co site. (2) CO interacts with $O_t$ atoms bonding to the V site, forming a nonlinear $CO_2$ unit. (3) Another O atom from $O_2$ or other oxidants can be added to V site to complete the proposed catalytic cycle. (See Figure 5.) Our results suggest a mechanism for a V−Co oxide catalyst surface enhancing the CO to $CO_2$ oxidation reaction.

## CONCLUSIONS

In conclusion, we generate neutral bimetallic oxide clusters for the first time. Experimental studies suggest that $VCoO_4$ can react with CO to produce $VCoO_3$ and $CO_2$. DFT calculations illustrate that the approaching of CO to the Co site, and the subsequent interaction of CO with one $O_t$ atom of the $O_bO_bVO_tO_t$ moiety of the $VCoO_4$ cluster is crucial to complete


dx.doi.org/10.1021/jz3008276 | J. Phys. Chem. Lett. 2012, 3, 2415−2419

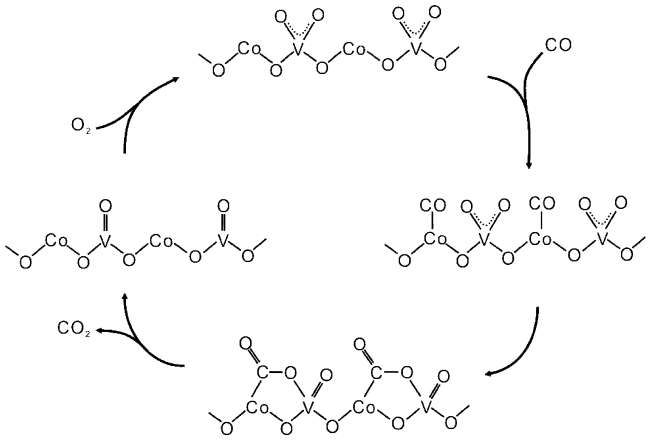

**Figure 5.** Proposed full catalytic cycle for CO oxidation to $CO_2$ on a V−Co oxide surface based on the calculations for the reaction of $VCoO_4$ cluster with CO.

the CO oxidation process. Our studies and results illuminate the mechanism for catalytic processes occurring on the surfaces of real supported catalysts, and suggest new types of multicomponent catalysts.

## ■ ASSOCIATED CONTENT

### Supporting Information

The optimzed low-lying isomers of $VCoO_4$ and $VCoO_3$ clusters and triplet potential energy surface for the reaction of $VCoO_4$ (**6**) with CO. This material is available free of charge via the Internet at http://pubs.acs.org.

## ■ AUTHOR INFORMATION

### Corresponding Author

*E-mail: erb@lamar.colostate.edu.

### Notes

The authors declare no competing financial interest.

## ■ ACKNOWLEDGMENTS

This work is partially supported by grants from the U.S. Air Force Office of Scientific Research (AFOSR) through grant number FA9550-10-1-0454 and the NSFERC for Extreme Ultraviolet Science and Technology under NSF Award No. 0310717.

## ■ REFERENCES

(1) Deo, G.; Wachs, I. E.; Haber, J. Supported Vanadium-Oxide Catalysts - Molecular Structural Characterization And Reactivity Properties. *Crit. Rev. Surf. Chem.* **1994**, *4*, 141−187.

(2) Reina, T. R.; Moreno, A. A.; Ivanova, S.; Odriozola, J. A.; Centeno, M. A. Influence of Vanadium or Cobalt Oxides on the CO Oxidation Behavior of Au/$MO_x$/$CeO_2$-$Al_2O_3$ Systems. *ChemCatChem* **2012**, *4*, 512−520.

(3) Concepcion, P.; Blasco, T.; Nieto, J. M. L.; Vidal-Moya, A.; Martinez-Arias, A. Preparation, Characterization and Reactivity of V- and/or Co-Containing AlPO-18 Materials (VCoAPO-18) in the Oxidative Dehydrogenation Of ethane. *Micropor. Mesopor. Mater.* **2004**, *67*, 215−227.

(4) Oliva, C.; Cappelli, S.; Rossetti, I.; Ballarini, N.; Cavani, F.; Forni, L. EPR Enlightening some Aspects of Propane ODH over $VO_x$-$SiO_2$ and $VO_x$-$Al_2O_3$. *Chem. Eng. J.* **2009**, *154*, 131−136.

(5) Wang, C. M.; Tsai, T. C.; Wang, I. Deep Hydrodesulfurization over Co/Mo Catalysts Supported on Oxides Containing Vanadium. *J. Catal.* **2009**, *262*, 206−214.

(6) Chen, J. H.; Shi, W. B.; Yang, S. J.; Arandiyan, H.; Li, J. H. Distinguished Roles with Various Vanadium Loadings Of $CoCr_{2-x}V_xO_4$ ($x$ = 0−0.20) for Methane Combustion. *J. Phys. Chem. C* **2011**, *115*, 17400−17408.

(7) Molinari, J. E.; Wachs, I. E. Presence of Surface Vanadium Peroxo-oxo Umbrella Structures in Supported Vanadium Oxide Catalysts: Fact or Fiction? *J. Am. Chem. Soc.* **2010**, *132*, 12559−12561.

(8) van Lingen, J. N. J.; Gijzernan, O. L. J.; Weckhuysen, B. M.; van Lenthe, J. H. On the Umbrella Model for Supported Vanadium Oxide Catalysts. *J. Catal.* **2006**, *239*, 34−41.

(9) Schwarz, H. Chemistry with Methane: Concepts Rather than Recipes. *Angew. Chem., Int. Ed.* **2011**, *50*, 10096−10115.

(10) Shi, Y.; E. R. Bernstein. Gas Phase Chemistry of Neutral Metal Clusters: Distribution, Reactivity and Catalysis *Int. J. Mass Spectrom.* **2012**, in press. DOI:10.1016/j.ijms.2012.06.001.

(11) Böhme, D. K.; Schwarz, H. Gas-Phase Catalysis by Atomic and Cluster Metal Ions: The Ultimate Single-Site Catalysts. *Angew. Chem., Int. Ed.* **2005**, *44*, 2336−2354.

(12) Zhai, H.-J.; Zhang, X.-H.; Chen, W.-J.; Huang, X.; Wang, L.-S. Stoichiometric and Oxygen-Rich $M_2O_n^-$ and $M_2O_n$ ($M$ = Nb, Ta; $n$ = 5−7) Clusters: Molecular Models for Oxygen Radicals, Diradicals, and Superoxides. *J. Am. Chem. Soc.* **2011**, *133*, 3085−3094.

(13) Wang, Z.-C.; Weiske, T.; Kretschmer, R.; Schlangen, M.; Kaupp, M.; Schwarz, H. Structure of the Oxygen-Rich Cluster Cation $Al_2O_7^+$ and Its Reactivity toward Methane and Water. *J. Am. Chem. Soc.* **2011**, *133*, 16930−16937.

(14) Ricks, A. M.; Gagliardi, L.; Duncan, M. A. Uranium Oxo and Superoxo Cations Revealed Using Infrared Spectroscopy in the Gas Phase. *J. Phys. Chem. Lett.* **2011**, *2*, 1662−1666.

(15) Kwapien, K.; Sierka, M.; Dobler, J.; Sauer, J.; Haertelt, M.; Fielicke, A.; Meijer, G. Structural Diversity and Flexibility of MgO Gas-Phase Clusters. *Angew. Chem., Int. Ed.* **2011**, *50*, 1716−1719.

(16) Roithová, J.; Schröder, D. Selective Activation of Alkanes by Gas-Phase Metal Ions. *Chem. Rev.* **2010**, *110*, 1170−1211.

(17) Jiang, L.; Wende, T.; Claes, P.; Bhattacharyya, S.; Sierka, M.; Meijer, G.; Lievens, P.; Sauer, J.; Asmis, K. R. Electron Distribution in Partially Reduced Mixed Metal Oxide Systems: Infrared Spectroscopy of $Ce_mV_nO_o^+$ Gas-Phase Clusters. *J. Phys. Chem. A* **2011**, *115*, 11187−11192.

(18) Santambrogio, G.; Janssens, E.; Li, S. H.; Siebert, T.; Meijer, G.; Asmis, K. R.; Dobler, J.; Sierka, M.; Sauer, J. Identification of Conical Structures in Small Aluminum Oxide Clusters: Infrared Spectroscopy of $(Al_2O_3)_{1-4}$(AlO). *J. Am. Chem. Soc.* **2008**, *130*, 15143−15149.

(19) Wang, Z.-C.; Dietl, N.; Kretschmer, R.; Weiske, T.; Schlangen, M.; Schwarz, H. Catalytic Redox Reactions in the CO/$N_2O$ System Mediated by the Bimetallic Oxide-Cluster Couple $AlVO_3^+$/$AlVO_4^+$. *Angew. Chem., Int. Ed.* **2011**, *50*, 12351−12354.

(20) Wang, Z.-C.; Wu, X.-N.; Zhao, Y.-X.; Ma, J.-B.; Ding, X.-L.; He, S.-G. Room-Temperature Methane Activation by a Bimetallic Oxide Cluster $AlVO_4^+$. *Chem. Phys. Lett.* **2010**, *489*, 25−29.

(21) Ding, X.-L.; Wu, X.-N.; Zhao, Y.-X.; He, S.-G. C-H Bond Activation by Oxygen-Centered Radicals over Atomic Clusters. *Acc. Chem. Res.* **2012**, *45*, 382−390.

(22) Reveles, J. U.; Johnson, G. E.; Khanna, S. N.; Castleman, A. W., Jr. Reactivity Trends in the Oxidation of CO by Anionic Transition Metal Oxide Clusters. *J. Phys. Chem. C* **2010**, *114*, 5438−5446.

(23) Zhang, Z.-G.; Xu, H.-G.; Kong, X.-Y.; Zheng, W.-J. Anion Photoelectron Spectroscopy and Density Functional Study of Small Aluminum-Vanadium Oxide Clusters. *J. Phys. Chem. A* **2011**, *115*, 13−18.

(24) Li, S. G.; Zhai, H. J.; Wang, L. S.; Dixon, D. A. Structural and Electronic Properties of Reduced Transition Metal Oxide Clusters, $M_3O_8$ and $M_3O_8^-$ ($M$ = Cr, W), from Photoelectron Spectroscopy and Quantum Chemical Calculations. *J. Phys. Chem. A* **2009**, *113*, 11273−11288.

(25) Zhai, H. J.; Wang, L. S. Probing the Electronic Structure and Band Gap Evolution of Titanium Oxide Clusters $(TiO_2)_n^-$ ($n$ = 1−10) Using Photoelectron Spectroscopy. *J. Am. Chem. Soc.* **2007**, *129*, 3022−3026.

(26) Zhai, H. J.; Döbler, J.; Sauer, J.; Wang, L. S. Probing the Electronic Structure of Early Transition-Metal Oxide Clusters: Polyhedral Cages of $(V_2O_5)_n^-$ ($n$ = 2−4) and $(M_2O_5)_2^-$ ($M$ = Nb, Ta). *J. Am. Chem. Soc.* **2007**, *129*, 13270−13276.
(27) Zhai, H. J.; Wang, L. S. Probing the Electronic Properties of Dichromium Oxide Clusters $Cr_2O_n^-$ ($n$ = 1−7) Using Photoelectron Spectroscopy. *J. Chem. Phys.* **2006**, *125*, 164315.
(28) Zhuang, J.; Li, Z. H.; Fan, K. N. A.; Zhou, M. F. Matrix Isolation Spectroscopic and Theoretical Study of Carbon Dioxide Activation by Titanium Oxide Molecules. *J. Phys. Chem. A* **2012**, *116*, 3388−3395.
(29) Zhou, M. F.; Zhou, Z. J.; Zhuang, J.; Li, Z. H.; Fan, K. N.; Zhao, Y. Y.; Zheng, X. M. Carbon Dioxide Coordination and Activation by Niobium Oxide Molecules. *J. Phys. Chem. A* **2011**, *115*, 14361−14369.
(30) Xie, Y.; Dong, F.; Heinbuch, S.; Rocca, J. J.; Bernstein, E. R. Oxidation Reactions on Neutral Cobalt Oxide Clusters: Experimental and Theoretical Studies. *Phys. Chem. Chem. Phys.* **2010**, *12*, 947−959.
(31) Dong, F.; Heinbuch, S.; Xie, Y.; Rocca, J. J.; Bernstein, E. R. Reactions of Neutral Vanadium Oxide Clusters with Methanol. *J. Phys. Chem. A* **2009**, *113*, 3029−3040.
(32) Dong, F.; Heinbuch, S.; Xie, Y.; Rocca, J. J.; Bernstein, E. R.; Wang, Z.-C.; Deng, K.; He, S.-G. Experimental and Theoretical Study of the Reactions Between Neutral Vanadium Oxide Clusters and Ethane, Ethylene, and Acetylene. *J. Am. Chem. Soc.* **2008**, *130*, 1932−1943.
(33) Dong, F.; Heinbuch, S.; He, S. G.; Xie, Y.; Rocca, J. J.; Bernstein, E. R. Formation and Distribution of Neutral Vanadium, Niobium, and Tantalum Oxide Clusters: Single Photon Ionization at 26.5 eV. *J. Chem. Phys.* **2006**, *125*, 164318.
(34) Johnson, G. E.; Mitrić, R.; Nössler, M.; Tyo, E. C.; Bonačić-Koutecký, V.; Castleman, A. W., Jr. Influence of Charge State on Catalytic Oxidation Reactions at Metal Oxide Clusters Containing Radical Oxygen Centers. *J. Am. Chem. Soc.* **2009**, *131*, 5460−5470.
(35) Li, Z.-Y.; Zhao, Y.-X.; Wu, X.-N.; Ding, X.-L.; He, S.-G. Methane Activation by Yttrium-Doped Vanadium Oxide Cluster Cations: Local Charge Effects. *Chem.—Eur. J.* **2011**, *17*, 11728−11733.
(36) Matsuda, Y.; Shin, D. N.; Bernstein, E. R. On the Copper Oxide Neutral Cluster Distribution in the Gas Phase: Detection Through 355 and 193 nm Multiphoton and 118 nm Single Photon Ionization. *J. Chem. Phys.* **2004**, *120*, 4165−4171.
(37) Matsuda, Y.; Shin, D. N.; Bernstein, E. R. On the Zirconium Oxide Neutral Cluster Distribution in the Gas Phase: Detection Through 118 nm Single Photon, and 193 and 355 nm Multiphoton, Ionization. *J. Chem. Phys.* **2004**, *120*, 4142−4149.
(38) He, S. G.; Xie, Y.; Guo, Y.; Bernstein, E. R. Formation, Detection, and Stability Studies of Neutral Vanadium Sulfide Clusters. *J. Chem. Phys.* **2007**, *126*, 194315.
(39) Matsuda, Y.; Bernstein, E. R. Identification, Structure, and Spectroscopy of Neutral Vanadium Oxide Clusters. *J. Phys. Chem. A* **2005**, *109*, 3803−3811.
(40) Matsuda, Y.; Bernstein, E. R. On the Titanium Oxide Neutral Cluster Distribution in the Gas Phase: Detection through 118 nm Single-Photon and 193 nm Multiphoton Ionization. *J. Phys. Chem. A* **2004**, *109*, 314−319.
(41) Xue, W.; Wang, Z.-C.; He, S.-G.; Xie, Y.; Bernstein, E. R. Experimental and Theoretical Study of the Reactions between Small Neutral Iron Oxide Clusters and Carbon Monoxide. *J. Am. Chem. Soc.* **2008**, *130*, 15879−15888.
(42) Dong, F.; Heinbuch, S.; Xie, Y.; Bernstein, E. R.; Rocca, J. J.; Wang, Z. C.; Ding, X. L.; He, S. G. C═C Bond Cleavage on Neutral $VO_3(V_2O_5)_n$ Clusters. *J. Am. Chem. Soc.* **2009**, *131*, 1057−1066.
(43) Wang, Z.-C.; Xue, W.; Ma, Y.-P.; Ding, X.-L.; He, S.-G.; Dong, F.; Heinbuch, S.; Rocca, J. J.; Bernstein, E. R. Partial Oxidation of Propylene Catalyzed by $VO_3$ Clusters: A Density Functional Theory Study. *J. Phys. Chem. A* **2008**, *112*, 5984−5993.
(44) He, S.-G.; Xie, Y.; Dong, F.; Heinbuch, S.; Jakubikova, E.; Rocca, J. J.; Bernstein, E. R. Reactions of Sulfur Dioxide with Neutral Vanadium Oxide Clusters in the Gas Phase. II. Experimental Study Employing Single-Photon Ionization. *J. Phys. Chem. A* **2008**, *112*, 11067−11077.
(45) Heinbuch, S.; Dong, F.; Rocca, J. J.; Bernstein, E. R. Experimental and Theoretical Studies of Reactions of Neutral Vanadium and Tantalum Oxide Clusters with NO and $NH_3$. *J. Chem. Phys.* **2010**, *133*, 174314.
(46) Zhao, Y.-X.; Wu, X.-N.; Ma, J.-B.; He, S.-G.; Ding, X.-L. Experimental and Theoretical Study of the Reactions between Vanadium-Silicon Heteronuclear Oxide Cluster Anions with n-Butane. *J. Phys. Chem. C* **2010**, *114*, 12271−12279.
(47) Ma, J. B.; Wu, X. N.; Zhao, Y. X.; Ding, X. L.; He, S. G. Methane Activation by $V_3PO_{10}^+$ and $V_4O_{10}^+$ Clusters: a Comparative Study. *Phys. Chem. Chem. Phys.* **2010**, *12*, 12223−12228.
(48) Ding, X. L.; Zhao, Y. X.; Wu, X. N.; Wang, Z. C.; Ma, J. B.; He, S. G. Hydrogen-Atom Abstraction From Methane by Stoichiometric Vanadium-Silicon Heteronuclear Oxide Cluster Cations. *Chem.—Eur. J.* **2010**, *16*, 11463−11470.
(49) Wang, Z.-C.; Wu, X.-N.; Zhao, Y.-X.; Ma, J.-B.; Ding, X.-L.; He, S.-G. C-H Activation on Aluminum−Vanadium Bimetallic Oxide Cluster Anions. *Chem.—Eur. J.* **2011**, *17*, 3449−3457.
(50) Dietl, N.; Höckendorf, R. F.; Schlangen, M.; Lerch, M.; Beyer, M. K.; Schwarz, H. Generation, Reactivity towards Hydrocarbons, and Electronic Structure of Heteronuclear Vanadium Phosphorous Oxygen Cluster Ions. *Angew. Chem., Int. Ed.* **2011**, *50*, 1430−1434.
(51) Zhang, Z.-G.; Xu, H.-G.; Zhao, Y.-C.; Zheng, W.-J. Photoelectron Spectroscopy and Density Functional Theory Study of $TiAlO_y^-$ ($y$ = 1−3) and $TiAl_2O_y^-$ ($y$ = 2−3) Clusters. *J. Chem. Phys.* **2010**, *133*, 154314.
(52) Nossler, M.; Mitric, R.; Bonacic-Koutecky, V.; Johnson, G. E.; Tyo, E. C.; Castleman, A. W., Jr. Generation of Oxygen Radical Centers in Binary Neutral Metal Oxide Clusters for Catalytic Oxidation Reactions. *Angew. Chem., Int. Ed.* **2010**, *49*, 407−410.
(53) Jakubikova, E.; Rappé, A. K.; Bernstein, E. R. Density Functional Theory Study of Small Vanadium Oxide Clusters. *J. Phys. Chem. A* **2007**, *111*, 12938−12943.
(54) Breneman, C. M.; Wiberg, K. B. Determining Atom-Centered Monopoles from Molecular Electrostatic Potentials. The Need for High Sampling Density in Formamide Conformational Analysis. *J. Comput. Chem.* **1990**, *11*, 361−373.
(55) Mota, S.; Volta, J. C.; Vorbeck, G.; Dalmon, J. A. Selective Oxidation of n-Butane on a V-P-O Catalyst: Improvement of the Catalytic Performance under Fuel-Rich Conditions by Doping. *J. Catal.* **2000**, *193*, 319−329.